Title no. 109-S01

Experimental Studies on Confinement Effect of Steel Hoops in Concrete Columns

by Wei-Jian Yi, Peng Li, and Sashi K. Kunnath

Four reinforced concrete (RC) frame column specimens without an effective concrete cover were tested under constant axial compressive and cyclic lateral loading. The seismic behavior of the specimens under different loading paths and axial load levels are examined with the objective of understanding the effect of confining action on the column response. The hoop strains of lateral reinforcement at different column heights under cyclic loading were attained by means of eight strain gauges attached along the hoops. Additionally, the characteristics of strain distribution in the transverse reinforcement were investigated. Results of the testing in conjunction with the cyclic stress-strain relationship of steel and the confining stress and its distribution around the cross section were evaluated. Finally, the effect of the confining force of transverse reinforcement on the ductility demand of columns under cyclic loading is highlighted.

Keywords: axial load; column(s); confinement; ductility; transverse reinforcement.

INTRODUCTION

In displacement-based seismic design, the ductility of a reinforced concrete (RC) column is an important design parameter. While the estimation of yielding displacement is more straightforward, the calculation of ultimate displacement may be more challenging because the displacement ductility of the column depends on its section ductility and the ultimate strain of concrete directly affects section ductility. Furthermore, the ultimate strain of concrete is influenced by the degree of lateral confinement. Consequently, a number of researchers have focused their efforts on developing the stress-strain relationship of confined concrete[1] and also proposed several effective analytical models for the axial compression behavior of confined concrete.[2-5] Very little effort, however, has been directed toward examining the effect of transverse reinforcement and the resulting confining pressures on columns under eccentric compression loading.

This experimental investigation is aimed at understanding the distribution of stress and strain of the concrete column section under cyclic loads. The effects of the applied axial load level (P/P_0), loading path, and location of transverse reinforcement are analyzed. The strain changes in transverse reinforcement and their influence on concrete crushing is also examined. The experimental results reported in this paper can form the basis of developing new and advanced transverse reinforcement confining models for concrete columns.

RESEARCH SIGNIFICANCE

The role of transverse reinforcement in enhancing the ductility of concrete sections is well recognized. Although numerous experiments have been carried out on column sections in pure axial compression for different confinement configurations, considerably less effort has been dedicated to understanding the role of confining pressure under combined axial and flexural loading. A unique set of experiments have been performed in this research study, wherein the cover concrete was removed and the exposed reinforcements were instrumented at critical locations on the transverse reinforcement in the plastic region. Data from the testing provide valuable insight into the nature of the confining stress distribution under lateral loads that can be used in the development of models to represent the confining action of transverse reinforcement under cyclic loads.

EXPERIMENTAL PROCEDURE

Specimen design

Two measures were taken to ensure the veracity and validity of transverse reinforcement strain measurements: first, no concrete cover was provided, hence the outer surface of the transverse reinforcement was exposed to air; second, in the potential plastic region, the transverse reinforcement was made up of steel rings fabricated from a seamless steel tube. These two measures made strain gauge installation much easier and ensured the quality of installation.

A total of four specimens were tested, each with a circular cross section, a diameter D of 336 mm (13.2 in.), and constructed of concrete with a measured cube (150 mm [6 in.]) compressive strength of 25.4 MPa (3683 psi) at 28 days. Based on specifications in the Chinese design code of concrete structures, the axial compressive strength of the concrete cylinder, f_c' (150 x 150 x 450 mm [6 x 6 x 18 in.]) is 20.3 MPa (2943 psi)—approximately 80% of the cube compressive strength. All the column specimens were cast in the same batch. Six concrete cubes with a side of 150 mm (6 in.) were tested to evaluate the mean value of concrete strength.

The net height of the columns, H, is 1800 mm (70.86 in.), including the top enhanced region that is 400 x 400 x 500 mm (15.75 x 15.75 x 19.68 in.). Each specimen has a 2000 x 700 x 430 mm (78.74 x 27.56 x 16.93 in.) base (Fig. 1). There are eight HRB335 longitudinal reinforcing bars (diameter $\Phi = 14$ mm [0.55 in.]) with a yield strength f_y of 361 MPa (52,345 psi). In the potential plastic region, the hoop reinforcement consists of steel rings 336 x 7 x 8 mm (13.2 x 0.28 x 0.31 in.) (outer diameter x thickness x width). There are, in total, seven steel rings distributed along a length of 480 mm (18.9 in.) from the top of the base section. In the remaining region, the transverse reinforcement is

Wei-Jian Yi *is a Professor in the College of Civil Engineering at Hunan University, Changsha, People's Republic of China, where he received his BS, MS, and PhD. His research interests include performance-based seismic design, blast resistance design of concrete structures, structural damage detection and health monitoring, and durability of concrete.*

Peng Li *is a PhD Student in the College of Civil Engineering at Hunan University. He received his BS and MS from Wuhan University, Wuchang, Hubei, People's Republic of China. His research interests include performance-based seismic design of concrete structures and nonlinear analysis of concrete structures.*

Sashi K. Kunnath, *FACI, is a Professor of Structural Engineering in the Department of Civil and Environmental Engineering, University of California at Davis, Davis, CA, and holds a Distinguished Visiting Professorship at Hunan University. He is a member of ACI Committees 335, Composite and Hybrid Structures; 374, Performance-Based Seismic Design of Concrete Structures; 375, Performance-Based Design of Concrete Buildings for Wind Loads; and S803, Faculty Network Coordinating Committee. He received the ACI Structural Research Award in 2001. His research interests include performance-based seismic engineering, nonlinear modeling of structural behavior, fatigue and failure of structural materials, and experimental methods in support of model-based simulation.*
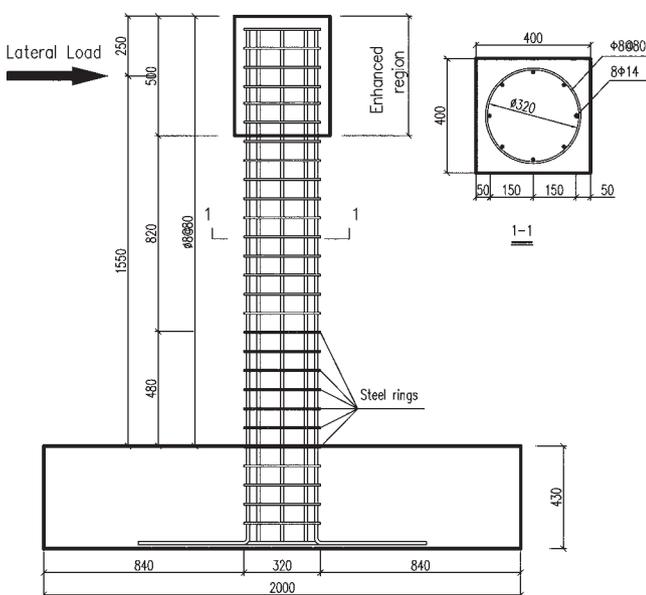
Fig. 1—Specimen details. (Note: Dimensions in mm; 1 mm = 0.0394 in.)

an HRB335 bar (diameter $\Phi = 8$ mm [0.31 in.], spacing = 80 mm [3.15 in.]). The model specimen is shown in Fig. 1 and the arrangement of strain gauges is shown in Fig. 2. In Fig. 2, CG refers to the transverse reinforcement gauges and "a" to "h" represent the location of the gauges.

Test setup and loading sequence

The experiment was carried out in the structural laboratory of Hunan University. A schematic drawing of the test setup is shown in Fig. 3. The specimen was mounted vertically with the bottom of the RC foundation resting on two steel beams. The end of the column was loaded by a hydraulic jack and controlled in a manner to provide a constant axial force of 450 and 900 kN (101 and 202 kips), corresponding to the axial load level P/P_0 of 0.2 and 0.4, respectively, in which P is the actual applied axial force and P_0 is calculated by the following equation

$$P_0 = f_c\left(A_g - A_s\right) + f_y A_s \qquad (1)$$

The column was subjected to reversed cyclic loading through an actuator mounted horizontally to a reaction wall. The actuator has a capacity of 600 kN (135 kips) and a maximum horizontal displacement of 250 mm (10 in.) in both positive and negative directions. The design load ratio of Specimens RC-1 and RC-2 is 0.2, whereas that of RC-3 and RC-4 is 0.4. All of the instrumented data are auto-recorded using the data acquisition system of the MTS controller.

The specimens were tested under displacement control. Two types of load paths were used: for Specimens RC-1 and RC-3, the displacement was increased by 5 mm (0.2 in.) (for example, a column drift of 0.32%) after three cycles at a specific drift. The displacement cycles were repeated in these tests to measure the strength degradation. For Specimens RC-2 and RC-4, the imposed displacement in the first step was 60 mm (2.36 in.), followed by decreasing displacements in decrements of 5 mm (0.2 in.) (Specimen RC-4) and 10 mm (0.4 in.) (Specimen RC-2) for subsequent cycles (without repetition). The displacement velocity in all tests was 1 mm/s (0.039 in./s).

TEST RESULTS
General observations

Because the specimens did not have a concrete cover, no cracking was observed on the outside tensile region until the longitudinal steel yield. The steel hoop did separate from the concrete in the tensile region during testing, however, which indicates the development of transverse cracks at the hoop locations or a bond failure. Concrete in the compression region was crushed after yielding of the transverse reinforcement. The failure mode is flexure for all specimens.

Hysteretic force-deformation response

The cyclic load-displacement relationships for Specimens RC-1 to RC-4 are shown in Fig. 4. The yielding of longitudinal steel bars, yielding of transverse reinforcement, and rupture of longitudinal steel bars for Specimens RC-1 and RC-3 are also indicated in the responses shown in Fig. 4. It can be seen from Fig. 4 that pinching of the hysteretic loops occurs for Specimens RC-1 and RC-3, and that transverse reinforcement yields after the yielding of the longitudinal steel bars. The rupture of the longitudinal bars is the last significant response event, and the load-carrying ability of the component degrades rapidly. Specimens RC-2 and RC-4 were subjected to decreasing displacement amplitudes, and less degradation in the response was observed, as there was less damage accumulation in the concrete and no longitudinal reinforcing steel bars ruptured.

Damage and inelastic behavior

The damaged state of the specimens is presented in Fig. 5, which shows the length of the plastic damage region. Crushing of the concrete in the plastic zone was much more severe in Specimen RC-1 than in RC-2, but in both cases, the damage length is approximately equal to one hoop spacing. The plastic damage length is estimated at two hoop spacings for Specimen RC-3, and it extends across three spacings in Specimen RC-4. This indicates that the length of the plastic damage region is not only a function of the axial stress and section ductility but also the loading history. A similar finding has been reported in tests conducted by El-Bahy et al.[6,7] When subjected to the same loading history, the length of the plastic region was found to increase with
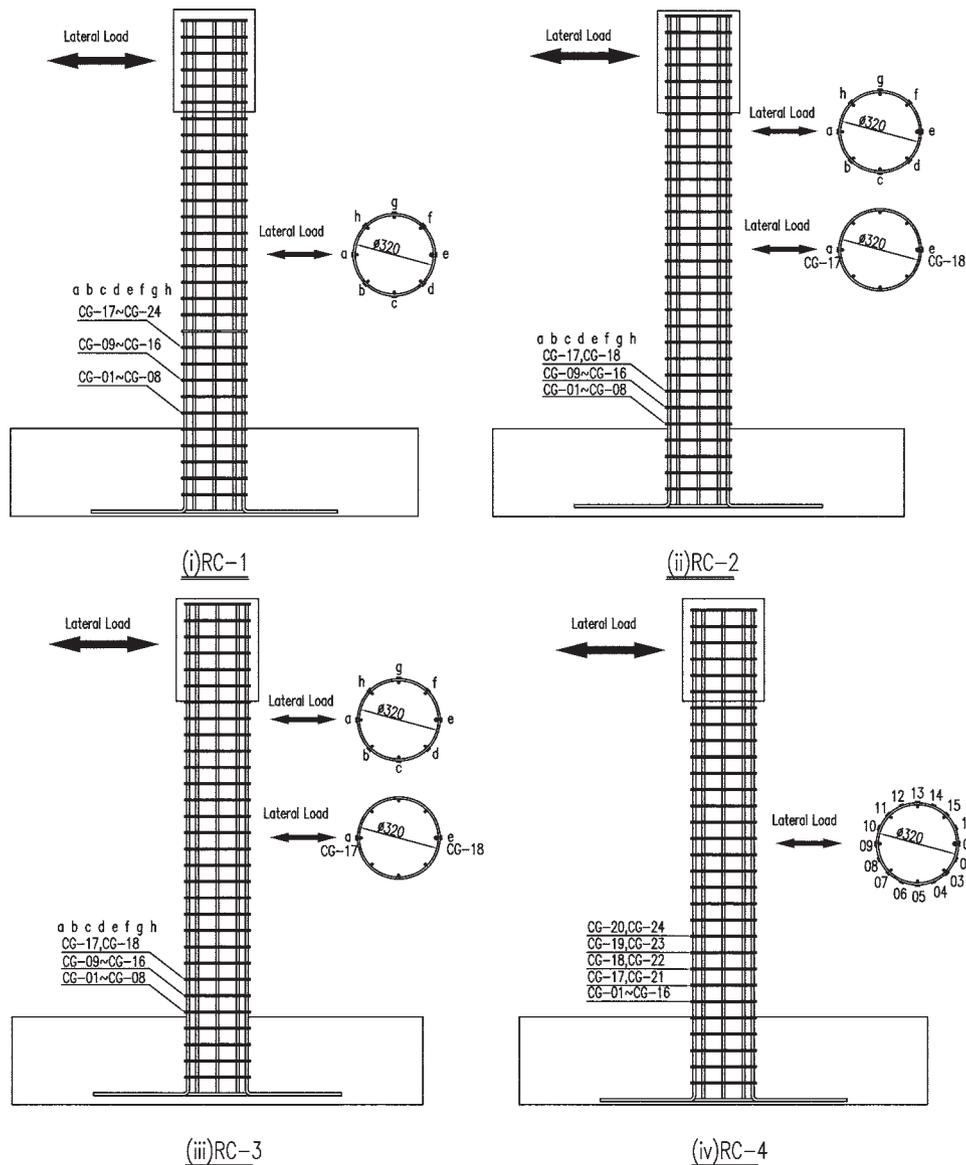
Fig. 2—Arrangement of gauges.

increasing axial stress. When considering Specimen RC-3, in which the load step increased gradually, the plastic region also grew gradually; however, the application of the high-amplitude inelastic displacement in the first cycle, followed by decreasing load steps, resulted in a larger plastic damage region in Specimen RC-4. Several researchers[8,9] and the AASHTO design provisions[10] have recommended that the estimation of plastic hinge length should consider the effect of axial load level.

Transverse reinforcement strains

The measurement of the strains in the transverse reinforcement can be considered the most significant aspect of this experiment. The strain distributions in the hoop, measured from the circumferentially arranged strain gauges (CG-1 to CG-8; refer to Fig. 2) in the first cycle of each displacement increment of Specimen RC-1, are plotted in Fig. 6(a). Likewise, the strain distributions in the hoop of Specimens RC-2, RC-3, and RC-4 are plotted in Fig. 6(b) to (d). It can be seen that in the beginning, the strain in the compression zone (Location 13# in Fig. 6(c)) increased, then decreased gradually as concrete crushing progressed;
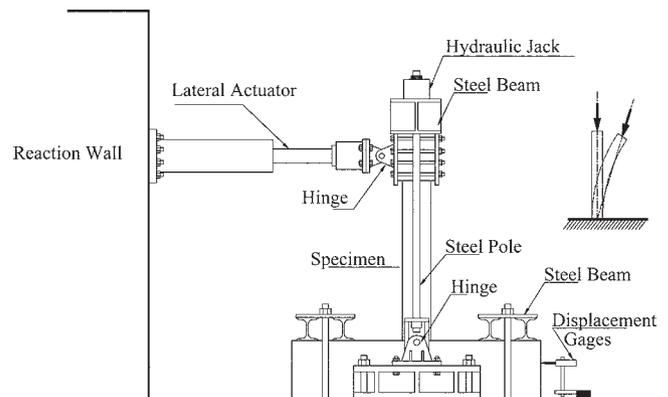
Fig. 3—Test setup.

on the other hand, the strain at Locations 12# and 14# increased constantly, indicating that the confinement action of the hoop at the compression zone (Location 13#) was lost when concrete failed, but the hoop continued to provide confinement at other positions. It is also observed from Fig. 6(c) that the strain on the tensile side of Specimen RC-3 (at Location 9#) attained a large value.
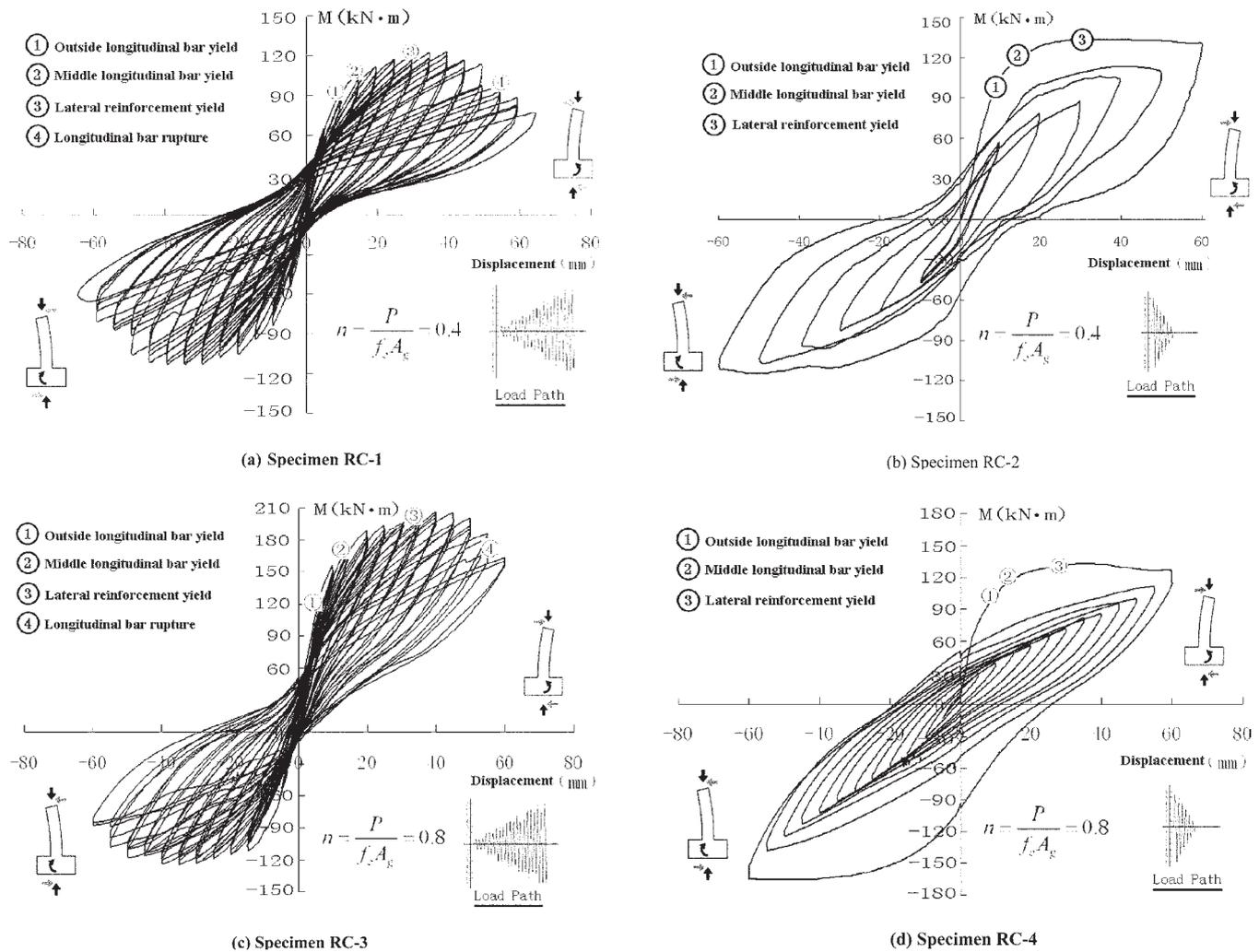
Fig. 4—Hysteretic load-displacement response of specimens. (Note: 1 mm = 0.0394 in.; 1 kN = 0.225 kips.)

There were 16 strain measurement points in the hoop of Specimen RC-4. The testing protocol for RC-4 was similar to RC-2 with the exception that the displacement decrement for RC-4 was half that of RC-2 (10 mm [0.4 in.] in each cycle as opposed to 5 mm [0.2 in.] for RC-4). It can be seen from Fig. 6(d) that, in general, the distributions of strain are similar; however, from the compression side to the tension side, the decrease in strain is more pronounced. When the cumulative displacement reached 20 mm (0.8 in.), the measured strain in the hoop was 2000 με, which indicated yielding of the hoop (refer to Table 1). Finally, the hoop strain along the height of the column is illustrated in Fig. 6(e), in which the strains on the compressive and tensile sides are plotted respectively on the right and left. The y-coordinate indicates the strain gauge number and the distance from the position of the measurement point to the base of the column, whereas the x-coordinate indicates the magnitude of strain in the hoops. As is evident from the figure, the strain increased rapidly at the location of the plastic region, but does not decrease consistently along the height. These observed distribution characteristics are identical with the test observations reported in similar research.[9,11,12] From Fig. 6 and test observations, the following findings are confirmed:

1. The lateral strain distribution is asymmetric. Before crushing of concrete, the lateral strain was tensile in both tensile and compression regions. This indicates that the hoop provides confinement to the entire concrete section.

2. When the concrete in the compression zone began crushing, the lateral strain did not decrease until concrete had spalled.

3. Compared with cyclic loading (refer to Fig. 6(a) and (c)), the strain in the steel hoops in the tensile section is larger than under monotonic loading (Fig. 6(b) and (d)) for the same load level. This suggests that the confining effect is influenced by the interaction between the steel hoops and concrete during cyclic loading.

Observations on recorded confining stresses

The computation of the confining stresses in the section requires information on the stress-strain relationship of the transverse reinforcement. Based on the stress-strain analysis of transverse reinforcement, Fig. 7 displays the confining stress distribution around the column section. Using the measured hoop strain in conjunction with the stress-strain model for reinforcing steel bars,[13] the circumferential stresses in the hoops can be calculated, following which the confining stress on the column surface can be obtained based on force equilibrium. These results are depicted in Fig. 7. There are two values for the confining stress: the value in parentheses refers to the confining stress in the weakly confined section (between the hoops) as calculated
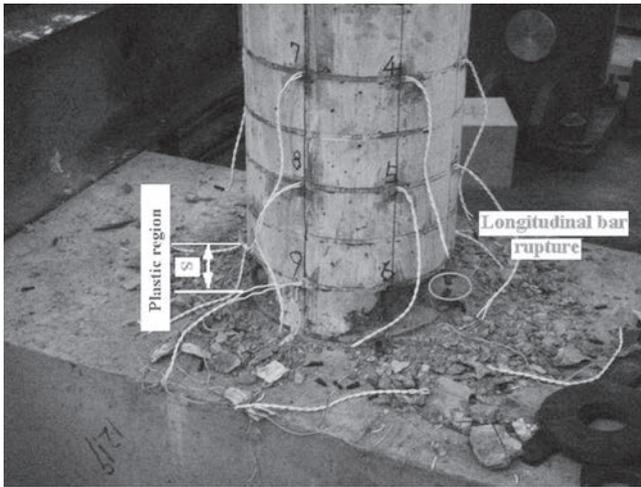
(a) Specimen RC-1
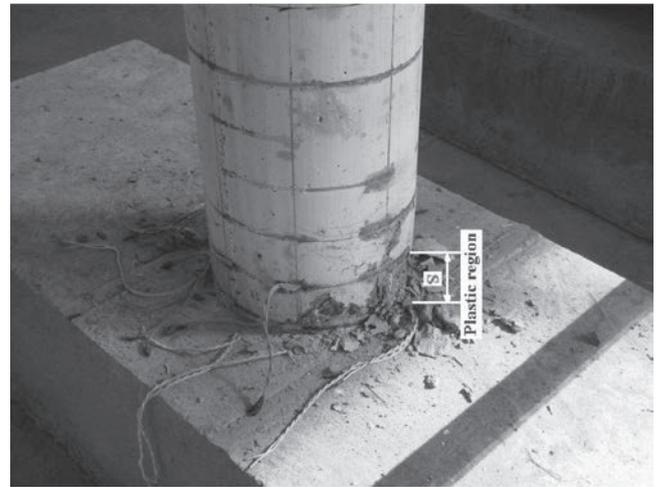
(b) Specimen RC-2

(c) Specimen RC-3

(d) Specimen RC-4

Fig. 5—Failure modes and plastic hinge region of specimens.

by Mander's confinement model,[2] and the other computed value of the confining stress is defined at the working position (the location of the steel hoop).

It can be seen from Fig. 7 that the confining stress distribution at the yield point is similar for all specimens and the confining stress in the tensile section has an approximately uniform distribution at yield. The yielding point and ultimate point are very close under the stepwise loading path, as in the case of Specimens RC-1 and RC-3. It is observed that the zone of transverse reinforcement yielding increases rapidly and the distribution of the confining stress is altered. At the ultimate point, the confining stress distribution of Specimen RC-4 is different from RC-1 and RC-3. There is no confining stress in the tensile section of RC-1 and RC-3 after concrete spalling. The concrete in the tensile section of RC-4 is still underconfined.

DISCUSSION AND ANALYSIS

Using the definition of yield and ultimate displacement introduced by Bae and Bayrak[11] (refer to Fig. 8), the displacement ductility factors for the tested specimens are listed in Table 2. It is observed that the displacement ductility factor of Specimen RC-3 is larger than that of Specimen RC-1 because the bending moment at the base

section of Specimen RC-3 does not drop markedly after reaching the peak load. Using the method proposed by Park and Paulay,[14] the following equations can be used to calculate the tip displacement of a column based on the "plastic hinge" concept

$$\Delta_u = \Delta_y + (\phi_u - \phi_y)l_p(l - 0.5l_p) \qquad (2)$$

$$\Delta_y = \frac{1}{3}\phi_y l^2 \qquad (3)$$

in which Δ_y and Δ_u are the yield and ultimate displacement, respectively; l is the calculated length of the column; ϕ_y is the yield curvature, which is estimated in this study from the measured yield displacement or sectional analysis; ϕ_u is the ultimate curvature, which can be obtained from sectional analysis; and l_p is the plastic hinge length. The displacement and curvature ductility factor are defined as $\mu_\Delta = \Delta_u/\Delta_y$ and $\mu_\phi = \phi_u/\phi_y$, respectively. The sectional analysis was carried out using a computer program coded by the authors based on the well-known fiber model approach. Concrete behavior is
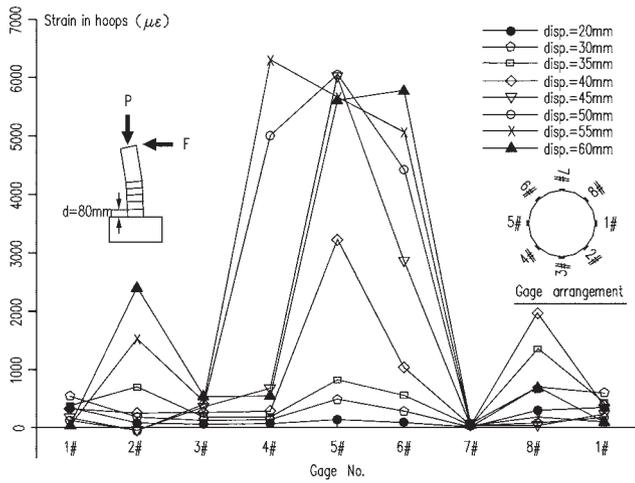
(a) Specimen RC-1
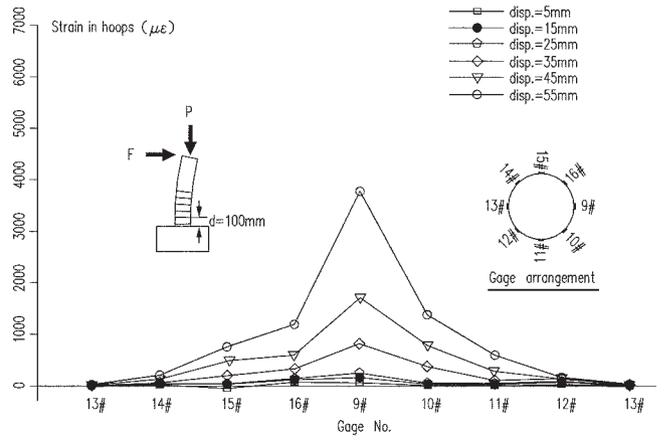
(b) Specimen RC-2
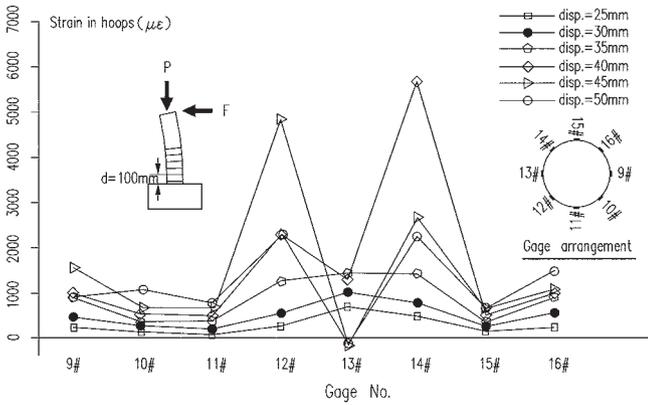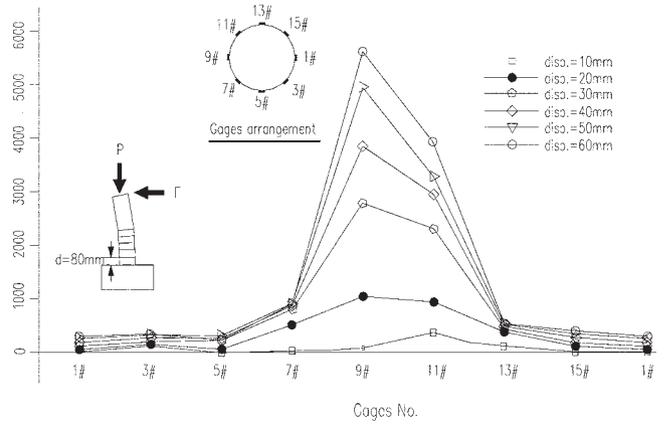
(c) Specimen RC-3
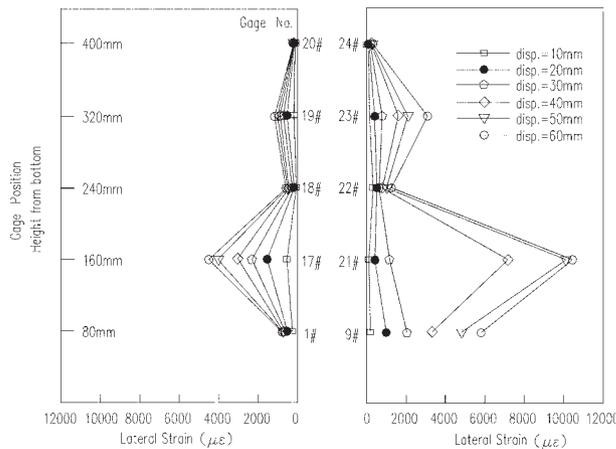
(d) Specimen RC-4

(e) Distribution along height of specimen RC-4

Fig. 6—Lateral strain distribution of specimens. (Note: 1 mm = 0.0394 in.)

Table 1—Main test results

Specimen	M_y, kN-m	Δ_y, mm	M_u, kN-m	Δ_u, mm	P/P_0*	μ_Δ
RC-1	100.9	13.8	97.0	50	0.40	3.62
RC-2	107.7	12.7	124.8	60*	0.40	—
RC-3	141.7	13.9	136.6	55	0.80	3.95
RC-4	125.2	10.4	150.7	60*	0.80	—

*Ultimate capacity of Specimens RC-2 and RC-4 did not drop significantly when their tip displacement reached 60 mm (2.36 in.)
Notes: 1 mm = 0.0394 in.; 1 kN-m = 0.74 kip-ft.

described through Mander's model.[2] Based on the confined stresses measured during testing (refer to Fig. 7), the actual stress-strain relationship for each fiber, referred to as the true state of "partial confinement" can also be determined. As further validation of the estimated demands, the software program COLUMNA[15] is also used for computation of the sectional curvature ductility of the columns. Because the COLUMNA[15] program cannot be used to compute the sectional deformation for partially confined concrete, values for the case of partial confinement are presented only for results obtained with the program developed by the authors.

(a) Specimen RC-1

(b) Specimen RC-3

(c) Specimen RC-4

Fig. 7—Confining stress distribution of specimens. (Note: 1 mm = 0.0394 in.; 1 kN = 0.225 kips.)
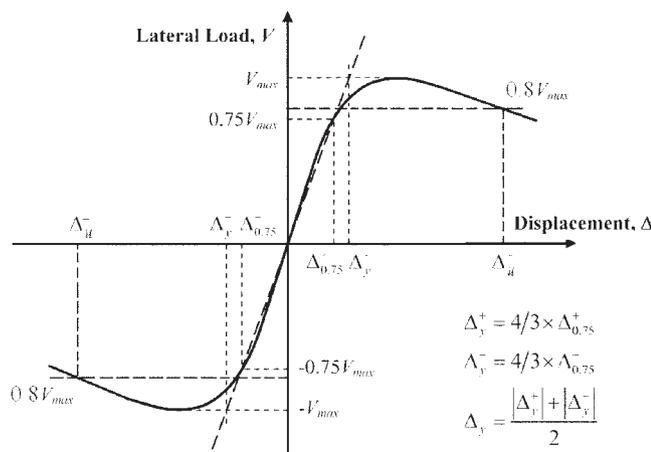
Fig. 8—Definition of yield displacement.[11]

Table 2—Material properties of specimens

No.	f_c', MPa	f_y, MPa	f_{yv}, MPa	f_{yv}', MPa	ρ_s, %	ρ_{sv}, %
RC-1 to RC-4	25.4	361.6	318.3	273.1	1.38	0.854

Notes: f_c' is concrete strength; f_y is longitudinal bar yielding strength; f_{yv} is transverse reinforcement yielding strength; f_{yv}' is steel ring yielding strength; ρ_x is longitudinal bar ratio; ρ_{sv} is transverse reinforcement volume ratio; 1 MPa = 0.145 ksi.

The yield curvature, ultimate curvature, and the curvature ductility of the section are listed in Table 3. The sectional ductility, based on partially confined stress distribution measured from the testing, is found to lie between that computed with the fully confined model and the unconfined model. To determine the displacement of the columns from the sectional curvature deformation, it is necessary to assume the length of the plastic hinge. The length of the plastic hinge suggested by Bae and Bayrak[12] is used

$$\frac{l_p}{h} = \left[0.3\left(\frac{P}{P_0}\right) + 3\left(\frac{A_s}{A_g}\right) - 0.1 \right]\left(\frac{L}{h}\right) + 0.25 \geq 0.25 \quad (4)$$

in which P/P_0 is the axial force ratio; A_s/A_g is the steel reinforcement ratio; and L/h is the shear-span ratio. Using Eq. (4), plastic hinge lengths of 179 mm (7 in.) (0.533D) and 365 mm (14.4 in.) (1.087D) are obtained for Columns RC-1 and RC-3, respectively. The yield displacement and ultimate displacements can subsequently be calculated by substituting the length of plastic hinge, yield curvature, and ultimate curvature into Eq. (2) and (3). The results obtained from the aforementioned calculations are listed in Table 4. It can be seen from Tables 1 and 4 that all the yield displacement values based on the three models are less than the measured values, with the largest deviation occurring for the unconfined model for both the yield and ultimate displacements. The calculated ultimate displacements using the fully confined model are significantly larger than the measured values; the results obtained with the partially confined model are seen to produce the closest estimates compared to the observed experimental values.

Based on the previous evaluation, it is shown that it is necessary to use a partially confined model to more accurately predict the displacement ductility of a cyclically loaded RC column. The nature of the confining stresses needs to be estimated based on experimental testing. The findings presented in this paper demonstrate the need to consider a more realistic distribution of confining stresses and the experimental data presented provide an initial basis for the development of a new confinement model.

CONCLUSIONS

Based on the experimental simulation of four specimens under cyclic loading, the effect of axial load level and loading path on the confining stress distribution in RC columns is investigated. It is found that both the axial load level and the loading path affect the length of the plastic region. The length of the plastic region increased as the axial load level increased. Prior to the crushing of concrete, the transverse reinforcement was found to provide confining stress both in the tensile and compressive sections. The strains in the transverse reinforcement increase rapidly after it yields, and the peak lateral load is achieved at this stage. After the concrete in the compression region is crushed, the lateral

Table 3—Sectional ductility estimates

	No.	ϕ_y,[*] rad/in.	ϕ_y,[†] rad/in.	ϕ_u,[*] rad/in.	ϕ_u,[†] rad/in.	μ_ϕ[*]	μ_ϕ[†]
RC-1	Confined	0.00031	0.00032	0.0048	0.0048	15.5	15.0
	Unconfined	0.00031	0.00031	0.0018	0.0019	5.8	6.13
	Partly confined	0.00034	—	0.0035	—	10.3	—
RC-3	Confined	0.00030	0.00029	0.0033	0.0032	11.0	11.03
	Unconfined	0.00030	0.00027	0.0009	0.0009	3.0	3.91
	Partly confined	0.00032	—	0.0021	—	6.6	—

[*]Calculated with program developed by the authors.
[†]Calculated with program COLUMNA.[15]
Note: 1 in. = 25.4 mm.

Table 4—Displacement ductility estimates

	No.	Δ_y, mm	Δ_u, mm	l_p, mm	μ_Δ	Error in displacement ductility estimate
RC-1	Confined	10.07	56.16	179	5.58	+54%
	Unconfined	9.76	26.12	179	2.68	−26%
	Partly confined	11.02	43.42	179	3.94	+9%
RC-3	Confined	9.13	66.28	365	7.26	+83%
	Unconfined	7.24	20.40	365	2.82	−29%
	Partly confined	10.39	45.15	365	4.35	+10%

Note: 1 mm = 0.0394 in.

strain does not decrease until concrete has spalled. In the plastic region, the maximum lateral strain is not correlated to the section location. The peak lateral strain occurred in the second or third spacing of the transverse reinforcement. At the base of the columns, the lateral strains are usually smaller because of additional confinement provided by the base foundation block.

The asymmetric distribution of the confining stress under combined axial force and cyclic bending indicates that it is essential to consider the nature of the confining stress distribution when calculating the moment-curvature relationship of the section. Because the degree of confinement varies with both the magnitude and history of applied loads, the estimation of section ductility should account for the true nature of the confining stresses. Compared with reversed cyclic loading, the strain in the steel hoops is lower under monotonic loading for the same displacement level. This suggests that the confining effect is influenced by the interaction between the steel hoops and concrete due to cyclic loading. Improved models that represent the true confining action in columns during cyclic loading are needed to better predict the displacement ductility of confined RC columns.

REFERENCES
1. Sheikh, S. A., and Uzumeri, S. M., "Strength and Ductility of Tied Concrete Columns," *Journal of the Structural Division*, ASCE, V. 106, May 1980, pp. 1079-1102.

2. Mander, J. B.; Priestley, M. J. N.; and Park, R., "Theoretical Stress-Strain Model for Confined Concrete," *Journal of Structural Engineering*, ASCE, V. 114, Aug. 1988, pp. 1804-1826.

3. Zhenhai, G., and Xudong, S., *Reinforced Concrete: Theory and Analyses*, Tsinghua University Press, Beijing, China, 2003, 345 pp. (in Chinese)

4. Zhenhai, G., and Chuangzhi, W., "Investigation of Strength and Failure Criterion of Concrete under Multi-Axial Stresses," *China Civil Engineering Journal*, V. 24, No. 3, 1991, pp. 1-14. (in Chinese)

5. Elwi, A. A., and Murray, D. W., "A 3D Hypoelastic Concrete Constitutive Relationship," *Journal of the Engineering Mechanics Division*, ASCE, V. 105, No. 4, Apr. 1979, pp. 623-641.

6. El-Bahy, A.; Kunnath, S. K.; Stone, W. C.; and Taylor, A. W., "Cumulative Seismic Damage of Circular Bridge Columns: Benchmark and Low-Cycle Fatigue Tests," *ACI Structural Journal*, V. 96, No. 4, July-Aug. 1999, pp. 633-641.

7. El-Bahy, A.; Kunnath, S. K.; Stone, W. C.; and Taylor, A. W., "Cumulative Seismic Damage of Circular Bridge Columns: Variable Amplitude Tests," *ACI Structural Journal*, V. 96, No. 5, Sept.-Oct. 1999, pp. 711-719.

8. Saatcioglu, M., and Baingo, D., "Circular High-Strength Concrete Columns under Simulated Seismic Loading," *Journal of Structural Engineering*, ASCE, V. 125, No. 3, Mar. 1999, pp. 272-280.

9. Bayrak, O., and Sheikh, S., "Plastic Hinge Analysis," *Journal of Structural Engineering*, ASCE, V. 127, No. 9, Sept. 2001, pp. 1092-1100.

10. AASHTO, "Standard Specifications for Highway Bridges," 16th edition, Division I-A: Seismic Design, American Association of State Highway and Transportation Officials, Washington, DC, 1995, 760 pp.

11. Bae, S., and Bayrak, O., "Seismic Performance of Full-Scale Reinforced Concrete Columns," *ACI Structural Journal*, V. 105, No. 3, May-June 2008, pp. 123-133.

12. Bae, S., and Bayrak, O., "Plastic Hinge Length of Reinforced Concrete Columns," *ACI Structural Journal*, V. 105, No. 3, May-June 2008, pp. 290-300.

13. Brown, J., and Kunnath, S. K., "Low-Cycle Fatigue Behavior of Reinforcing Steel Bars," *ACI Materials Journal*, V. 101, No. 6, Nov.-Dec. 2004, pp. 457-466.

14. Park, R., and Paulay, T., *Reinforced Concrete Structures*, John Wiley & Sons, Inc., New York, 1975, 769 pp.

15. Kuebitz, K. C., "Development and Calibration of COLUMNA, a Windows®-Based Moment-Curvature Program for Columns of Arbitrary Cross Sections," MS thesis, University of California-San Diego, San Diego, CA, 2002, 454 pp.